

# Strange Hadron Production in Au+Au Collisions at RHIC Beam Energy Scan

Yingjie Zhou<sup>1,\*</sup> (for the STAR Collaboration)

<sup>1</sup>Key Laboratory of Quark & Lepton Physics (MOE) and Institute of Particle Physics, Central China Normal University, Wuhan 430079, China

**Abstract.** Strangeness production has been suggested to be a sensitive probe to the early-time dynamics of the nuclear matter created in heavy-ion collisions. Transverse momentum distributions and yields of strange hadrons provide important information on their production mechanisms and can help us probe the properties of the created medium and its evolution.

Thanks to the high statistics data taken during the STAR BES-II program in 2018-2021, a series of measurements on the properties of strangeness production at low energies are carried out. In these proceedings, the production of  $K^-$ ,  $K_S^0$ ,  $\phi$ ,  $\Lambda$ , and  $\Xi^-$  in Au+Au collisions at  $\sqrt{s_{NN}} = 3$  GeV are presented. The strange hadron transverse momentum spectra, rapidity density distributions, and particle ratios are shown. These results are compared with UrQMD model calculations, and the extracted kinetic freeze-out parameters are discussed and compared with the ones from higher collision energies.

## 1 Introduction

The main goal of the STAR experiment is to study the properties of the QCD matter under extreme conditions, i.e., high temperature and high density, by colliding heavy ions at ultra-relativistic speed. The yields and particle ratios of strange hadrons provide important information about their production mechanisms in these collisions. The RHIC Beam Energy Scan (BES) program covers a wide range of energies to explore the transition from a hadronic dominated phase to a partonic dominated one. Of particular interest is the high baryon density region which is accessible through the STAR fixed-target (FXT) program covering the energy range from 13.7 GeV down to 3 GeV.

## 2 Data Analysis

In these proceedings, we focus on results obtained from FXT Au+Au collisions at  $\sqrt{s_{NN}} = 3$  GeV recorded in 2018. In total, approximately 260M minimum bias events are used in this analysis. Particle identification (PID) is performed using the energy loss ( $dE/dx$ ) information from Time Projection Chamber (TPC) and the particle velocity ( $\beta$ ) information from Time of Flight (TOF). Short-lived particles are reconstructed via their hadronic decay channels, using the KF Particle Finder package [1] which is based on the Kalman Filter method. The combinatorial background is estimated with the rotating daughter method, in

---

\*e-mail: yingjiezhou@mails.ccnu.edu.cn

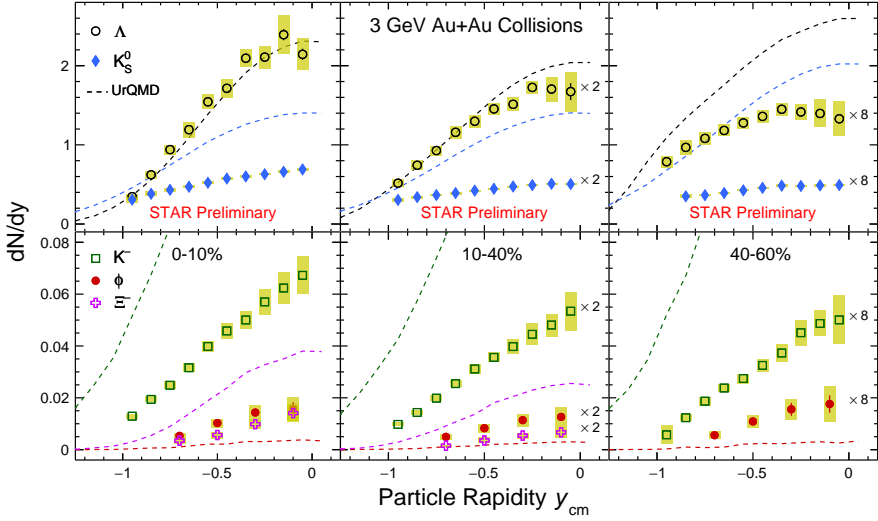


**Figure 1.** The rapidity dependence of  $dN/dy$  of  $\Lambda$ ,  $K_S^0$ ,  $K^-$ ,  $\phi$  and  $\Xi^-$  in Au+Au collisions at  $\sqrt{s_{NN}} = 3$  GeV in different centralities. The yields at 10-40% and 40-60% are scaled up by a factor of 2 and 8 respectively for better visibility. The vertical lines and bands represent the statistical and systematic uncertainties. The dashed lines are the calculations from UrQMD.

36 which a daughter track of the  $K_S^0$ ,  $\Lambda$  and  $\Xi^-$  is rotated by a random angle between 150 to 210  
 37 degrees in the transverse plane. For  $\phi$  meson, the combinatorial background is estimated by  
 38 the mixing event technique.

### 39 **3 Results and Discussion**

#### 40 **3.1 Centrality and Rapidity Dependence of Yields of Strange Particles**

41 The transverse momentum ( $p_T$ ) spectra of  $\Lambda$  and  $K_S^0$  are extrapolated to the unmeasured re-  
 42 gion with several fitting functions (such as blast-wave function,  $m_T$  exponential, etc.) to ob-  
 43 tain the  $p_T$ -integrated yields in different rapidity and centrality regions. The  $dN/dy$  of  $\Lambda$  and  
 44  $K_S^0$  in different centrality intervals are shown in Fig. 1, and are compared with other strange  
 45 particles,  $K^-$ ,  $\phi$ , and  $\Xi^-$  [2], and UrQMD calculations [3]. For  $\Lambda$ , UrQMD reproduces the  
 46 measured rapidity distributions in central collisions, but overestimates the data in peripheral  
 47 collisions. UrQMD significantly overestimates the  $K^-$ ,  $K_S^0$ , and  $\Xi^-$  yields, and underestimates  
 48 the  $\phi$  yields. To gain more insight on the production of strange baryons, the ratio of the  $\Lambda$   
 49 yield to the proton yield is presented in Fig. 2, as a function of rapidity and centrality. The  
 50  $\Lambda/p$  ratio exhibits clear rapidity and centrality dependence, whose shape can be qualitatively  
 51 described by UrQMD. An enhancement of  $\Lambda/p$  ratio is observed at mid-rapidity compared to  
 52 target rapidity, likely due to an increase in hadronic interactions from target to mid-rapidity.

#### 53 **3.2 Dependence of Strangeness Production on Number of Participating Nucleons**

54 The total strange hadron yields divided by the mean number of participants ( $\langle N_{part} \rangle$ ) is shown  
 55 in Fig. 3 as a function of  $\langle N_{part} \rangle$ . For comparison, the proton yields are also shown. The

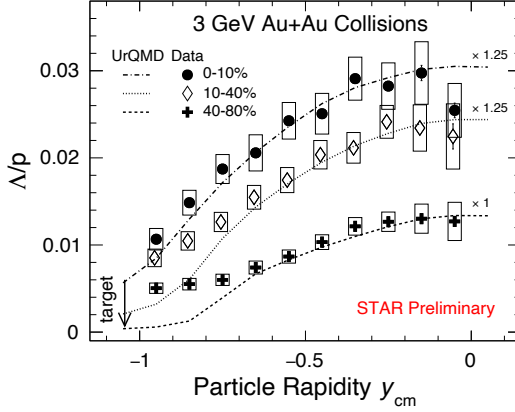


**Figure 2.** Rapidity dependence of  $\Lambda/p$  for different centrality bins in Au+Au collisions at  $\sqrt{s_{NN}} = 3$  GeV. Vertical lines represent statistical uncertainties, while boxes represent systematic uncertainties. 10-40% centrality is shifted left for better visibility. The curves represent the calculations from UrQMD and are scaled up to compare with data.

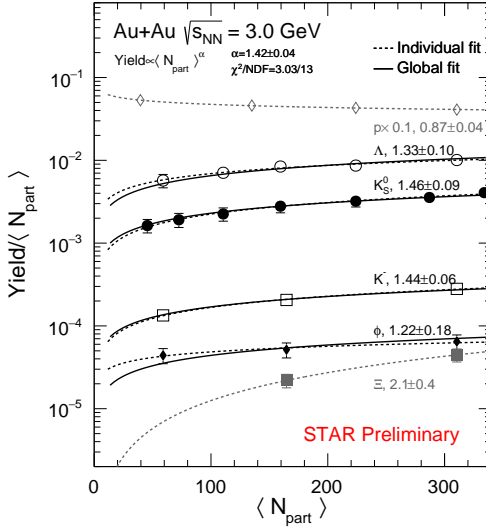


**Figure 3.** Hadron yields per mean number of participants as a function of  $\langle N_{part} \rangle$ . All hadron yields are fitted with a function of the form  $f \propto C \langle N_{part} \rangle^\alpha$  shown as black dash lines, and the fitted  $\alpha$  values are shown in the figures. The black solid lines represent a simultaneous fit to all strange hadron yields ( $K^-$ ,  $K_S^0$ ,  $\Lambda$ ,  $\phi$ ).

56 hadron yields are fitted with the function  $dN/dy \propto C \langle N_{part} \rangle^\alpha$  and the slope parameter  $\alpha$  is  
57 extracted for each particle separately. The extracted slope parameters for  $K^-$ ,  $K_S^0$ ,  $\Lambda$ , and  
58  $\phi$  are consistent with each other, indicating universal centrality dependence of strangeness  
59 production in  $\sqrt{s_{NN}} = 3$  GeV collisions. A combined fit to all four strange hadrons gives  
60  $\alpha = 1.42 \pm 0.04$ . In contrast to strange particles, the yield of protons divided by  $\langle N_{part} \rangle$   
61 decreases with centrality. It is also interesting to note here that the slope parameter of  $\Xi^-$   
62 is  $2.1 \pm 0.4$ , which deviates from the scaling trend. This could be due to the fact that  $\Xi^-$  is  
63 produced below its  $NN$  threshold, 3.25 GeV, while the  $NN$  production thresholds of the other  
64 strange particles ( $K^-$ ,  $K_S^0$ ,  $\Lambda$ , and  $\phi$ ) lie below  $\sqrt{s_{NN}} = 3$  GeV. The precise measurement of  
65  $\Xi^-$  yield will be carried out with the additional 2 billion Au+Au events on tape.

### 66 3.3 Kinetic Freeze-out Properties

67 The spectra of  $p$ ,  $\Lambda$  and  $K_S^0$  at  $\sqrt{s_{NN}} = 3$  GeV are fitted with a boost-invariant blast-wave  
68 model [4] which assumes a radially boosted thermal source. The fit parameters, i.e. effective

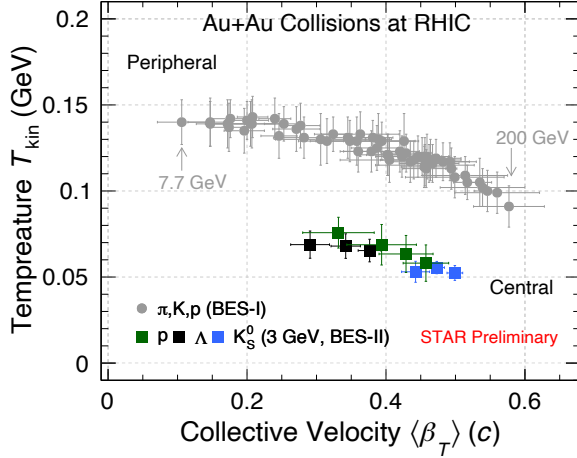


**Figure 4.** Effective temperature  $T_{\text{kin}}$  vs collective velocity  $\langle\beta_T\rangle$  for  $p$  (green),  $\Lambda$  (black) and  $K_S^0$  (blue) extracted from blast-wave fits at  $\sqrt{s_{\text{NN}}} = 3$  GeV. The fit parameters for  $(\pi, K, p)$  from  $\sqrt{s_{\text{NN}}} = 7.7$  to 200 GeV are shown for comparison.

69 temperature  $T_{\text{kin}}$  and collective velocity  $\langle\beta_T\rangle$ , are obtained and shown in Fig. 4.  $\langle\beta_T\rangle$  increases  
70 from peripheral to central collisions for all three particles. We observe that  $T_{\text{kin}}$  of  $\Lambda$  is  
71 systematically higher than that of  $K_S^0$  at  $\sqrt{s_{\text{NN}}} = 3$  GeV. The results are compared to those  
72 obtained from  $(\pi, K, p)$  spectra in  $\sqrt{s_{\text{NN}}} = 7.7$  to 200 GeV Au+Au collisions [5]. The  $T_{\text{kin}}$  of  
73  $p, \Lambda$  and  $K_S^0$  are significantly lower compared to higher energy collisions.

## 74 4 Summary

75 In summary, measurements on strangeness production in 3 GeV Au+Au collisions have  
76 been discussed. Yields of  $\Lambda$  and  $K_S^0$  have been presented as a function of rapidity and  
77 centrality. The measured strange particle yields are inconsistent with UrQMD calculations.  
78 The yields of all strange particles except for  $\Xi^-$  scale with  $\langle N_{\text{part}} \rangle$  to the power  $\alpha$ , where  
79  $\alpha = 1.42 \pm 0.04$ , indicating universal strangeness production as a function of centrality. The  
80 apparent deviation of  $\Xi^-$  from this trend could be due to the fact that at  $\sqrt{s_{\text{NN}}} = 3$  GeV,  $\Xi^-$   
81 is produced below its  $NN$  production threshold. Finally, blast-wave fits to  $\Lambda$  and  $K_S^0$  spectra  
82 result in a lower effective kinetic freeze-out temperature compared to that of  $\pi, K, p$  spectra  
83 at  $\sqrt{s_{\text{NN}}} = 7.7$  GeV or higher.

84  
85 **Acknowledgement:** This work was supported in part by the National Key Research and Development  
86 Program of China under Grant No. 2020YFE0202002, and the Fundamental Research Funds for the  
87 Central Universities (Nos. CCNU22QN005, CCNU20TS005).

## 88 References

- 89 [1] K. I., J. Phys. Conf. Ser. 1 p. 602 (2020)  
90 [2] M.S. Abdallah et al. (STAR), Phys. Lett. B **827**, 137003 (2022)  
91 [3] S.A. Bass et al., Prog. Part. Nucl. Phys. **41**, 255 (1998)  
92 [4] E. Schnedermann, J. Sollfrank, U. Heinz, Physical Review C **48**, 2462 (1993)  
93 [5] L. Adamczyk et al. (STAR), Phys. Rev. C **96**, 044904 (2017)